Low-Birefringent and Highly Tough Nanocellulose-Reinforced Cellulose Triacetate

Hiroto Soeta,[†] Shuji Fujisawa,[‡] Tsuguyuki Saito,[†] Lars Berglund,[§] and Akira Isogai*,[†]

[†]Department of Biomaterials Science, Graduate School of Agricultural and Life Sciences, The University of Tokyo, Tokyo 113-8657, Japan

[‡]Department of Biomass Chemistry, Forestry and Forest Products Research Institute, 1 Matsuno-sato, Tsukuba, Ibaraki 305-8687, Japan

[§]Fibre and Polymer Technology, School of Chemical Science and Engineering, Royal Institute of Technology, Teknikringen 56-58, SE-100 44, Stockholm, Sweden

S *Supporting Information*

ABSTRACT: Improvement of the mechanical and thermal properties of cellulose triacetate (CTA) films is required without sacrificing their optical properties. Here, poly(ethylene glycol) (PEG)-grafted cellulose nanofibril/CTA nanocomposite films were fabricated by casting and drying methods. The cellulose nanofibrils were prepared by 2,2,6,6-tetramethylpiperidine-1-oxyl (TEMPO)-mediated oxidation, and amine-terminated PEG chains were grafted onto the surfaces of the TEMPO-oxidized cellulose nanofibrils (TOCNs) by ionic

	Neat cellulose triacetate (CTA)	2.5% nanocellulose/ CTA composite
Haze (%)	0.2	1.5
Retardation (nm)	40	47
Toughness (MJ/m^3)	11	46

bonds. Because of the nanosize effect of TOCNs with a uniform width of ∼3 nm, the PEG−TOCN/CTA nanocomposite films had high transparency and low birefringence. The grafted PEG chains enhanced the filler−matrix interactions and crystallization of matrix CTA molecules, resulting in the Young's modulus and toughness of CTA film being significantly improved by PEG-grafted TOCN addition. The coefficient of thermal expansion of the original CTA film was mostly preserved even with the addition of PEG-grafted TOCNs. These results suggest that PEG−TOCNs are applicable to the reinforcement for transparent optical films.

KEYWORDS: *nanocellulose, cellulose triacetate, TEMPO, birefringence, nanocomposite*

INTRODUCTION

Cellulose and its derivatives are used as paper and board, textiles, plastics, thickeners, and additives in various commodity and high-value material fields. Cellulose triacetate (CTA), a cellulose derivative, is used as films in optical devices, hollow fibers in seawater desalination systems, and so on. In particular, CTA is widely used as protective films for polarizing plates and supporting films for liquid crystal displays. The CTA film has high transparency and low birefringence, and is tougher and lighter than glasses.[1,2] For its further applications, improvements in the mechanical and thermal properties of CTA are required by film thinning, weight saving, and enhancing the thermal stability of CTA in the assembly process. Either increasing the crystallinity of the polymer or incorporating rigid inorganic fillers is often used to improve the properties of polymeric materials. However, these methods cause a significant decrease in the optical transparency of the polymer films and increase the birefringence. Although some studies of CTA/filler composites have been reported,[3−6] the birefringence of such reinforced CTA composites has not been revealed. Reinforcement that can preserve both the transparency and birefringence of CTA is required.

In recent years, cellulose has attracted attention as nanoscale fibers. In nature, cellulose forms highly crystalline and few nanometer-wide fibrils, which are called cellulose microfibrils.[7] Plant cellulose microfibrils combine high aspect ratio and excellent mechanical properties.[8−10] Because of these properties, cellulose microfibrils are a promising candidate for polymer reinforcement materials.[12−16] A high aspect ratio of the microfibrils and sufficient dispersibility in matrices is necessary for effective reinforcement, although it is generally difficult to homogeneously disperse high-aspect-ratio cellulose microfibrils in polymer matrices.

Cellulose microfibrils with high aspect ratio can be isolated from wood cellulose fibers by 2,2,6,6-tetramethylpiperidine-1-oxyl (TEMPO)-mediated oxidation and mechanical treatment of the oxidized celluloses in water.[17,18] Isolated microfibrils, or TEMPO-oxidized cellulose nanofibrils (TOCNs), have a uniform width of ∼3 nm, high aspect ratios >100, and a high density of carboxylate groups on the TOCN surfaces. TOCN/polymer composites have been prepared and show better

mechanical properties than the original polymers.[19−23] TOCNs can be dispersed in not only water but also a variety of organic solvents by modifying the counterions of the surface carboxylate groups,[24,25] which may allow sufficient nano-dispersion of the TOCNs in various hydrophilic and hydrophobic polymers. The nanocomposites thus obtained show improved mechanical properties without sacrificing the optical properties of the original polymers, because of the nanodispersibility and favorable TOCN−polymer interactions caused by the surface modification of TOCNs.[26,27] Therefore, TOCNs have great potential as nanofillers for effective reinforcement of transparent polymer films.

In this study, we prepared poly(ethylene glycol) (PEG)-grafted TOCN (PEG−TOCN)/CTA nanocomposite films to improve the mechanical and thermal properties of CTA films while retaining their original optical properties. The TOCN surfaces were selectively modified by PEG chains to improve the nanodispersibility in the CTA matrix. The nanocomposite films were prepared by mixing a PEG−TOCN/organic solvent dispersion and a CTA/organic solvent solution with various volume/volume ratios, and then casting and drying. The mechanical, optical, and thermal properties of the composite films were then investigated.

■ MATERIALS AND METHODS

Materials. A softwood bleached kraft pulp (SBKP) (Nippon Paper Industries Co. Ltd., Tokyo, Japan) was used to prepare the TOCNs. CTA (LT-35; degrees of polymerization and substitution are 270 and 2.87, respectively, from catalog data) was supplied by Daicel Corp., Tokyo, Japan. Amine-terminated PEG (PEG−NH₂, Sunbright MEPA-10H, M_w = 1085) was purchased from NOF Corp., Tokyo, Japan. Pure PEG (M_w = 1000, no amine groups) and other reagents and solvents of laboratory grade were purchased from Wako Pure Chemical Industries, Ltd., Osaka, Japan.

TEMPO-Mediated Oxidation. TEMPO-mediated oxidation was performed according to a previously reported method.[17] SBKP (1.0 g) was suspended in water (100 mL) containing TEMPO (0.016 g; 1 mM) and sodium bromide (0.1 g; 10 mM). Sodium hypochlorite solution (6.2 mL; 3.8 mmol g⁻¹ pulp) was added to the pulp/water slurry. The slurry was stirred at room temperature at pH 10. The TEMPO-oxidized cellulose (TOC) (1.0 g) was further treated with sodium chlorite (1.3 g) in 0.5 M acetate buffer (100 mL) at pH 4−5 and room temperature for 48 h to oxidize the residual C6-aldehyde groups to carboxylate groups. The carboxylate content of the oxidized cellulose was determined to be 1.13 mmol g⁻¹ by conductometric titration.

Preparation of PEG−TOCN/Chloroform Dispersion. A 0.1 wt % TOCN−COONa/water dispersion was prepared from the TEMPO-oxidized SBKP by mechanical disintegration treatment in water. The TOCN−COONa/water dispersion was converted to aqueous TOCN−COOH gel particles, and then the gel was converted to a 0.1 wt % PEG−TOCN/chloroform dispersion by sonication of the TOCN−COOH gel and PEG−NH₂ in CHCl₃ for 3 min, where the molar ratio of PEG−NH₂ to the carboxyl groups of TOCNs was adjusted to 1:1.[26] Here, stable dispersion of the TOCNs at the individual level in CHCl₃ was achieved by grafting the PEG chains densely on the TOCN surfaces via TOCN-carboxylate/PEG-ammonium ionic bonds.

Preparation of PEG−TOCN/CTA Nanocomposite Films. CTA was dissolved in dichloromethane at a concentration of 20 mg mL⁻¹. The CTA/CH₂Cl₂ solution and the PEG−TOCN/CHCl₃ dispersion were mixed at different ratios and stirred for 30 min. In the present study, the "TOCN content" is defined as the weight percent of TOCNs based on the total weight of each nanocomposite film without taking into account the grafted PEG weight. The mixture was casted in a glass Petri dish. The mixture of the CTA/CH₂Cl₂ solution and the

PEG−TOCN/CHCl₃ dispersion was dried at room temperature for 24 h.

Analysis. Light transmittance spectra of the films were measured from 350 to 850 nm with a spectrophotometer (V-670, JASCO Corp., Tokyo, Japan). The haze values of films with a thickness of about 80 μm were measured using an HZ-V3 haze meter (Suga Test Instruments Co., Ltd., Tokyo, Japan). Retardation of the nanocomposite films in the thickness direction was measured using a KOBRA-21ADH optical birefringence analyzer (Oji Scientific Instruments Co., Ltd., Hyogo, Japan) in low-phase-difference mode at 589.3 nm. The birefringence was measured at a light incidence angle of 40°. Tensile tests were carried out using a Shimadzu EZ-TEST tensile tester (Kyoto, Japan) equipped with a 500 N load cell. Specimens with a dimension of 40 × 3 mm² were measured at 20 mm min⁻¹ with a 10 mm span length, and at least five specimens were measured for each sample. Wide-angle X-ray diffraction (WAXD) patterns of the PEG−TOCN/CTA nanocomposite films were obtained using a Rigaku RINT2000 diffractometer with Cu Kα radiation (λ = 1.5418 Å) at 40 kV and 40 mA. Thermomechanical analysis was carried out at a 0.03 N load in a nitrogen atmosphere from 30 to 150 °C at 5 °C min⁻¹ using a Shimadzu thermomechanical analyzer (TMA-60, Shimadzu Corp., Kyoto, Japan), and the coefficients of thermal expansion (CTE) of the films were calculated.

■ RESULTS AND DISCUSSION

Fundamental Properties of PEG−TOCN/CTA Nanocomposite Films. In this study, CHCl₃ was used to prepare the PEG−TOCN dispersion, and CH₂Cl₂ was used as the solvent for CTA, because CH₂Cl₂ is a better solvent than CHCl₃ for CTA. No phase separation of the two components was observed during drying the mixtures to prepare the composite films, even though two different organic solvents were used in the film preparation. The film densities and water contents of the nanocomposite films are shown in Figure S1 in the Supporting Information. The film densities were almost constant at ∼1 g cm⁻³ at 23 °C and 50% relative humidity irrespective of the TOCN content, and the water content slightly decreased from 2% to 1.6% with increasing TOCN content from 0 to 2.5 wt %. This slight decrease in water content of the PEG−TOCN/CTA composite films will be discussed later. The content of the PEG moiety in the composite films linearly increased to 2.75 wt % with increasing TOCN content from 0 to 2.5 wt % (Figure S1 in the Supporting Information).

Optical Properties of PEG−TOCN/CTA Nanocomposite Films. The PEG−TOCN/CTA nanocomposite films were flexible and transparent (Figure 1b). The light transmittance of the nanocomposite film containing 2.5 wt % TOCNs was 90% at 600 nm, while that of the neat CTA film was 91% (Figure 1a). This result shows that the 3 nm-wide TOCNs can be homogeneously dispersed in the CTA matrix by PEG grafting.[26] As previously observed,[28−30] light scattering was effectively suppressed in the nanocomposite films.

The haze value is an indicator of the cloudiness of transparent materials, and is expressed as

$$\text{haze (\%)} = \frac{T_d}{T_t} 100 \tag{1}$$

where T_d is the deflected light transmittance and T_t is the total light transmittance. The haze value is defined as the percentage of light that is deflected more than 2.5° from the direction of the incident light. The haze values of films are explained in terms of two light scattering mechanisms: (1) light scattering caused by fillers present inside the film, and (2) that caused by roughness of the film surface morphology. Thus, the smoother
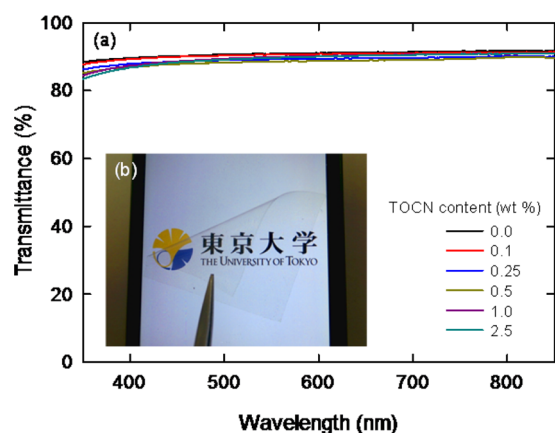
Figure 1. (a) Light transmittance of PEG−TOCN/CTA nano-composite films with various TOCN contents. (b) Photograph of the nanocomposite film containing 2.5 wt % TOCNs.

the film surface, the lower the haze value. Figure 2 shows the haze values of the PEG−TOCN/CTA nanocomposite films.
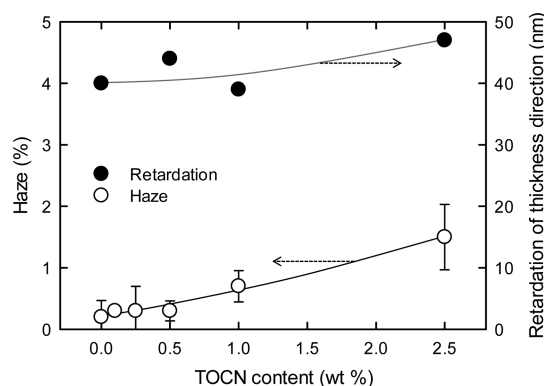

Figure 2. Haze value and retardation in the thickness direction (R_{th}) of PEG−TOCN/CTA nanocomposite films.

The haze value of the nanocomposite film containing 2.5 wt % TOCNs was 1.5%, whereas that of the neat CTA film was 0.2%. It has been reported that fillers can function as diffusion centers for visible light.[31] In this study, the PEG−TOCNs functioned as diffusion centers and the haze value slightly increased. However, the haze values of the nanocomposite films were still as small as those of conventional transparent films such as poly(methyl methacrylate) and poly(carbonate).[32] Moreover, the haze value can be further improved by tailoring the roughness of the film surfaces.[33]

Figure 2 also shows the retardation in the thickness direction (R_{th}) of the nanocomposite films. The retardation is defined as birefringence × film thickness. R_{th} values of 40−50 nm are typical for CTA films with a thickness of about 80 μm.[1] The R_{th} value of the neat CTA film was preserved even with the addition of 2.5 wt % TOCNs, although the cellulose crystal itself has optical anisotropy. In this study, the TOCN content in the nanocomposite films was very low. Therefore, it seems that the effect of anisotropic cellulose crystals on the retardation value of the nanocomposite films is negligible.

Mechanical Properties of PEG−TOCN/CTA Nano-composite Films. The Young's modulus, tensile strength, and elongation at break of the CTA films greatly improved with the addition of PEG−TOCNs (Figure 3a and b). As a result,
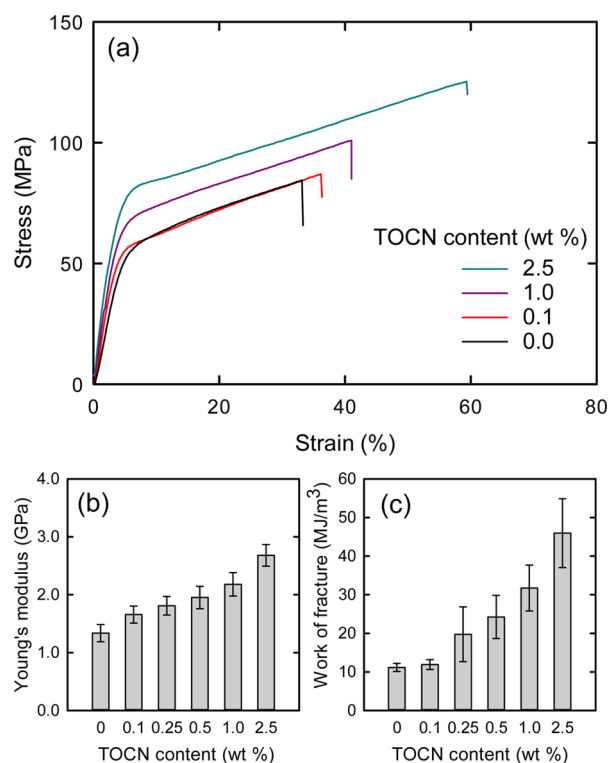

Figure 3. Mechanical properties of the PEG−TOCN/CTA nano-composite films: (a) stress−strain curves, (b) Young's moduli, and (c) work of fracture.

the work of fracture of the CTA films increased from 11.2 to 46.0 MJ m^{-3}, or by about 400%, as the PEG−TOCN content increased from 0 to 2.5 wt % (Figure 3c). This behavior is different from conventional cellulose nanofibril/polymer composite films.[18−21,27] Cellulose nanofibril/polymer composites generally becomes brittle with nanofibril addition. It has been reported that surface modification of carbon nanotubes increases the Young's modulus, breaking stress, ultimate tensile strength, and toughness of the resultant carbon nanotube/polymer composites. These improvements in the mechanical properties can be explained by enhancement in the interfacial shear strength between the polymer matrix and nanotubes by surface modification.[34] In the present study, it is likely that the grafted PEG chains also improved the TOCN/CTA interfacial shear strength, and as a result, the toughness of the nanocomposite films effectively increased.

Model Approach. A model was applied to evaluate the validity of the PEG−TOCN reinforcement. Assuming that the PEG−TOCNs were randomly dispersed in the CTA matrix, the Halpin−Tsai model,[35] as expressed in the following eq 2, was used to calculate the theoretical Young's moduli of the nanocomposites:

$$E_{HT} = \left[\frac{3}{8} \frac{1 + 2(l_f/d_f)\eta_L V_f}{1 - \eta_L V_f} + \frac{5}{8} \frac{1 + 2\eta_T V_f}{1 - \eta_T V_f} \right] E_m \quad (2)$$

where E_{HT} and E_m are the moduli of the composite and matrix, respectively, and l_f and d_f are the length and width of the filler, respectively. V_f is the volume fraction of fillers in the composite system. The V_f value of the TOCNs was calculated using the densities of TOCNs (1.6 g cm^{-3}) and CTA (1.28 g cm^{-3}).[2,36,37] η_L and η_T have the following expressions:

$$\eta_{\text{L}} = \frac{(E_{\text{fL}}/E_{\text{m}}) - 1}{(E_{\text{fL}}/E_{\text{m}}) + 2(l_{\text{f}}/d_{\text{f}})} \tag{3}$$

$$\eta_{\text{T}} = \frac{(E_{\text{fT}}/E_{\text{m}}) - 1}{(E_{\text{fT}}/E_{\text{m}}) + 2} \tag{4}$$

where E_{fL} and E_{fT} are the longitudinal and transverse moduli, respectively, of the filler. In this study, E_{m} of 1.33 GPa was used, which was determined from the tensile test data of the neat CTA film. For TOCNs, E_{fL} = 134 GPa,[8] E_{fT} = 24.8 GPa,[38] d_{f} = 3 nm,[26] and l_{f} = 1087 nm[39] were used. The Young's modulus of the nanocomposites is plotted against the volume fraction of TOCNs in Figure 4.
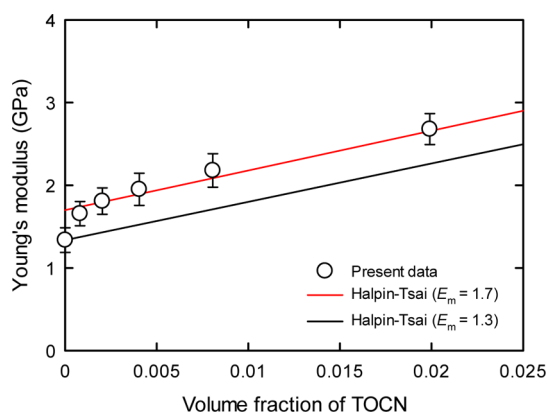

Figure 4. Experimentally obtained and calculated Young's modulus of the PEG−TOCN/CTA nanocomposite films versus the volume fraction of TOCNs.

The experimentally obtained Young's moduli were slightly higher than the theoretical moduli calculated using the model. When E_{m} is assumed to be 1.7 GPa, the Young's moduli of the PEG−TOCN/CTA nanocomposite films were almost consistent with those calculated using the model. This result indicates (1) the Young's modulus of the CTA matrix of the nanocomposites increased with PEG−TOCN addition, (2) the PEG−TOCNs were individually dispersed in the CTA matrix without agglomeration, and (3) the PEG−TOCNs interacted with CTA molecules. It is likely that the increase in E_{m} was caused by a slight increase in the crystallinity of the CTA matrix. This hypothesis is supported by the results of WAXD measurement (Figure 5). The neat CTA film had a typical WAXD pattern with low crystallinity, and had broad diffraction peaks around 2θ = 8.5, 16, and 21°.[40,41] In particular, the diffraction intensity and sharpness of the peak at 8.5° owing to CTA clearly increased with PEG−TOCN addition. This increase in the crystallinity of CTA with the PEG−TOCN addition may have resulted in a slight decrease in the water content of the PEG−TOCN/CTA nanocomposite films (Figure S1 in the Supporting Information).

Next, a model that quantitatively evaluates the interfacial interaction was used[42,43]

$$\ln \sigma_{\text{r}} = \ln \sigma_{\text{c}} \frac{1 + 2.5\varphi_{\text{f}}}{1 - \varphi_{\text{f}}} = \ln(\sigma_{\text{m}}) + B\varphi_{\text{f}} \tag{5}$$

where σ_{r} is the reduced yield strength, σ_{c} and σ_{m} are the yield strength of the composite and neat polymer, respectively, φ_{f} is the volume fraction of the filler, and B is a parameter related to interfacial interactions.[42,44,45] The yield strength was deter-
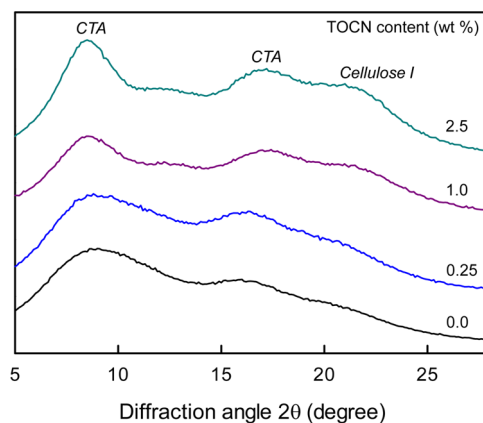

Figure 5. WAXD patterns of the PEG−TOCN/CTA nanocomposite films.

mined from the obtained stress−strain curves. In Figure 6, $\ln(\sigma_{\text{r}})$ is plotted against the volume fraction of TOCNs. The B
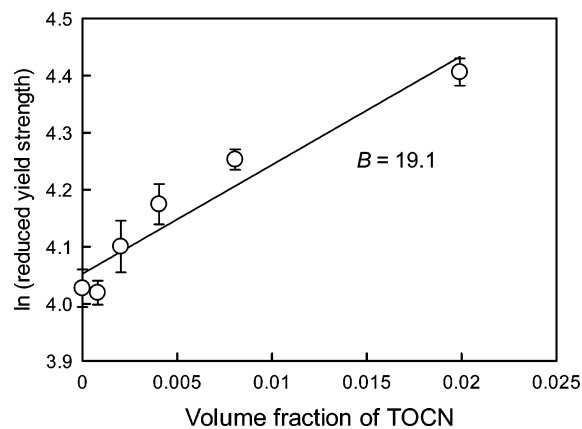

Figure 6. Reduced yield strength of the PEG−TOCN/CTA nanocomposite films versus the volume fraction of TOCNs.

value was calculated from the slope of the straight line in Figure 6. In this study, B = 19.1 (R^2 = 0.928), which is higher than the B values of previous studies for surface-treated $CaCO_3$/poly(propylene) (PP) composites, such as linear low-density poly(ethylene)/clay nanocomposites with compatibilizer, and surface-modified cellulose fiber/PP composite.[42−44,46−48] The large B value indicates some favorable interfacial interactions and good load transfer efficiency at the interface. The B value is influenced by many factors, such as the shape and aspect ratio of filler, filler dispersion, and interfacial interactions. In the present study, the large B value can be attributed to the high aspect ratio and nanodispersibility of TOCNs in the CTA matrix, and the increase in interactions between TOCN elements and CTA molecules by PEG grafting on the TOCNs.

Thermal Expansion Behavior of PEG−TOCN/CTA Nanocomposite Films. The CTE values of the PEG−TOCN/CTA nanocomposite films are shown in Figure 7. The CTE of the nanocomposite films was almost constant with TOCN addition of 0−2.5 wt %. In general, the addition of a rigid filler causes a significant reduction in the CTE, because the network of fillers restrains the thermal expansion of the polymer matrix.[27,49,50] In the case of the nanocomposites fabricated in this study, the rigid TOCNs likely suppressed the thermal expansion of the matrix, while the flexible PEG chains
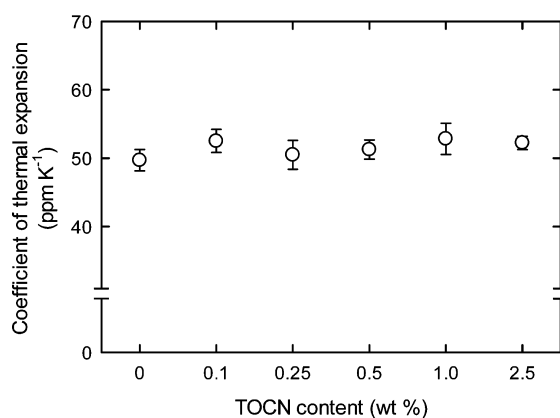
Figure 7. Coefficient of thermal expansion of the PEG–TOCN/CTA nanocomposite films.

caused an increase in the CTE of the nanocomposite films (Figure S3 in the Supporting Information). As a result, the effects of TOCNs and PEG canceled out, and the thermal dimensional stability of the neat CTA film did not change with addition of PEG–TOCNs.

CONCLUSIONS

PEG–TOCN/CTA nanocomposite films containing 0–2.5 wt % TOCNs were successfully prepared. Because of the nanosize effect of TOCNs, the high transparency and low birefringence of the original CTA films were mostly preserved in the nanocomposite films. In addition, the Young's modulus and toughness of the nanocomposites greatly improved with the addition of PEG–TOCNs. The reinforcing effect can be regarded as a result of the addition of surface-grafted PEG chains to CTA, which improve the filler–matrix interactions and crystallization of matrix CTA molecules. These results show that PEG–TOCNs are a promising nanofiller for the reinforcement of transparent optical materials.

ASSOCIATED CONTENT

ⓈSupporting Information

Densities and water contents of the PEG-TOCN/CTA nanocomposite films, and the mechanical and thermal expansion properties of PEG/CTA composite films. The Supporting Information is available free of charge on the ACS Publications website at DOI: 10.1021/acsami.5b02863.

AUTHOR INFORMATION

Corresponding Author
*E-mail: aisogai@mail.ecc.u-tokyo.ac.jp. Tel: +81 3 5841 5538. Fax: +81 3 5841 5269.

Notes
The authors declare no competing financial interest.

ACKNOWLEDGMENTS

REFERENCES

(1) Sata, H.; Murayama, M.; Shimamoto, S. Properties and Applications of Cellulose Triacetate Film. *Macromol. Symp.* **2004**, *208*, 323−333.

(2) Balser, K.; Hoppe, L.; Eicher, T.; Wandel, M.; Astheimer, H.-J.; Steinmeier, H.; Allen, J. M. Cellulose Esters. *Ullmann's Encycl. Ind. Chem.* **2012**, *7*, 333−380.

(3) Rajini, R.; Venkateswarlu, U. Studies on the Composites of Cellulose Triacetate (prepared from Sugar Cane Pulp) and Gelatin. *J. Appl. Polym. Sci.* **2001**, *82*, 847−853.

(4) Kim, Y. J.; Ha, S. W.; Jeon, S. M.; Yoo, D. W.; Chun, S. H.; Sohn, B. H.; Lee, J. K. Fabrication of Triacetylcellulose-SiO₂ Nanocomposites by Surface Modification of Silica Nanoparticles. *Langmuir* **2010**, *26*, 7555−7560.

(5) Basavaraja, C.; Jo, E. A.; Kim, B. S.; Huh, D. S. Electromagnetic Interference Shielding of Cellulose Triacetate/Multiwalled Carbon Nanotube Composite Films. *Polym. Compos.* **2011**.

(6) Basavaraja, C.; Jo, E. A.; Kim, B. S.; Huh, D. S. Thermal Stimulated Conductivity in Cellulose Triacetate-Multiwalled Carbon Nanotube Polymer Films. *Bull. Korean Chem. Soc.* **2010**, *31*, 2207−2210.

(7) Nishiyama, Y. Structure and Properties of the Cellulose Microfibril. *J. Wood Sci.* **2009**, *55*, 241−249.

(8) Sakurada, I.; Nukushima, Y.; Ito, T. Experimental Determination of Elastic Moduli of the Crystalline Regions in Oriented Polymers. *J. Polym. Sci.* **1962**, *57*, 651−660.

(9) Šturcová, A.; Davies, G. R.; Eichhorn, S. J. Elastic Modulus and Stress-Transfer Properties of Tunicate Cellulose Whiskers. *Biomacromolecules* **2005**, *6*, 1055−1061.

(10) Iwamoto, S.; Kai, W.; Isogai, A.; Iwata, T. Elastic Modulus of Single Cellulose Microfibrils from Tunicate Measured by Atomic Force Microscopy. *Biomacromolecules* **2009**, *10*, 2571−2576.

(11) Saito, T.; Kuramae, R.; Wohlert, J.; Berglund, L. a.; Isogai, A. An Ultrastrong Nanofibrillar Biomaterial: The Strength of Single Cellulose Nanofibrils Revealed via Sonication-Induced Fragmentation. *Biomacromolecules* **2013**, *14*, 248−253.

(12) Samir, M. A. S. A.; Alloin, F.; Dufresne, A. Review of Recent Research into Cellulosic Whiskers, Their Properties and Their Application in Nanocomposite Field. *Biomacromolecules* **2005**, *6*, 612−626.

(13) Hubbe, M. A.; Rojas, O. J.; Lucia, L. A.; Sain, M. Cellulosic Nanocomposites: A Review. *BioResources* **2008**, *3*, 929−980.

(14) Pandey, J. K.; Ahn, S. H.; Lee, C. S.; Mohanty, A. K.; Misra, M. Recent Advances in the Application of Natural Fiber Based Composites. *Macromol. Mater. Eng.* **2010**, *295*, 975−989.

(15) Eichhorn, S. J.; Dufresne, a.; Aranguren, M.; Marcovich, N. E.; Capadona, J. R.; Rowan, S. J.; Weder, C.; Thielemans, W.; Roman, M.; Renneckar, S.; Gindl, W.; Veigel, S.; Keckes, J.; Yano, H.; Abe, K.; Nogi, M.; Nakagaito, A. N.; Mangalam, A.; Simonsen, J.; Benight, A. S.; Bismarck, A.; Berglund, L. A.; Peijs, T. Review: Current International Research into Cellulose Nanofibres and Nanocomposites. *J. Mater. Sci.* **2010**, *45*, 1−33.

(16) Habibi, Y.; Lucia, L.; Rojas, O. Cellulose Nanocrystals: Chemistry, Selfassembling, and Applications. *Chem. Rev.* **2010**, *110*, 3479−3500.

(17) Saito, T.; Nishiyama, Y.; Putaux, J. L.; Vignon, M.; Isogai, A. Homogeneous Suspensions of Individualized Microfibrils from TEMPO-Catalyzed Oxidation of Native Cellulose. *Biomacromolecules* **2006**, *7*, 1687−1691.

(18) Isogai, A.; Saito, T.; Fukuzumi, H. TEMPO-Oxidized Cellulose Nanofibers. *Nanoscale* **2011**, *3*, 71−85.

(19) Li, Z.; Renneckar, S.; Barone, J. R. Nanocomposites Prepared by in Situ Enzymatic Polymerization of Phenol with TEMPO-Oxidized Nanocellulose. *Cellulose* **2010**, *17*, 57−68.

(20) Bulota, M.; Tanpichai, S.; Hughes, M.; Eichhorn, S. J. Micromechanics of TEMPO-Oxidized Fibrillated Cellulose Composites. *ACS Appl. Mater. Interfaces* **2012**, *4*, 331−337.

(21) Johnson, R. K.; Zink-Sharp, A.; Renneckar, S. H.; Glasser, W. G. A New Bio-Based Nanocomposite: Fibrillated TEMPO-Oxidized

Celluloses in Hydroxypropylcellulose Matrix. *Cellulose* **2009**, *16*, 227−238.

(22) Masoodi, R.; El-Hajjar, R. F.; Pillai, K. M.; Sabo, R. Mechanical Characterization of Cellulose Nanofiber and Bio-Based Epoxy Composite. *Mater. Des.* **2012**, *36*, 570−576.

(23) Besbes, I.; Vilar, M. R.; Boufi, S. Nanofibrillated Cellulose from Alfa, Eucalyptus and Pine Fibres: Preparation, Characteristics and Reinforcing Potential. *Carbohydr. Polym.* **2011**, *86*, 1198−1206.

(24) Okita, Y.; Fujisawa, S.; Saito, T.; Isogai, A. TEMPO-Oxidized Cellulose Nanofibrils Dispersed in Organic Solvents. *Biomacromolecules* **2011**, *12*, 518−522.

(25) Fujisawa, S.; Okita, Y.; Saito, T.; Togawa, E.; Isogai, A. Formation of *N*-Acylureas on the Surface of TEMPO-Oxidized Cellulose Nanofibril with Carbodiimide in DMF. *Cellulose* **2011**, *18*, 1191−1199.

(26) Fujisawa, S.; Saito, T.; Kimura, S.; Iwata, T.; Isogai, A. Surface Engineering of Ultrafine Cellulose Nanofibrils toward Polymer Nanocomposite Materials. *Biomacromolecules* **2013**, *14*, 1541−1546.

(27) Fujisawa, S.; Ikeuchi, T.; Takeuchi, M.; Saito, T.; Isogai, A. Superior Reinforcement Effect of TEMPO-Oxidized Cellulose Nanofibrils in Polystyrene Matrix: Optical, Thermal, and Mechanical Studies. *Biomacromolecules* **2012**, *13*, 2188−2194.

(28) Yano, H.; Sugiyama, J.; Nakagaito, a. N.; Nogi, M.; Matsuura, T.; Hikita, M.; Handa, K. Optically Transparent Composites Reinforced with Networks of Bacterial Nanofibers. *Adv. Mater.* **2005**, *17*, 153−155.

(29) Iwamoto, S.; Nakagaito, a. N.; Yano, H.; Nogi, M. Optically Transparent Composites Reinforced with Plant Fiber-Based Nanofibers. *Appl. Phys. A Mater. Sci. Process.* **2005**, *81*, 1109−1112.

(30) Dahman, Y.; Oktem, T. Optically Transparent Nanocomposite Reinforced With Modified Biocellulose Nnofibers. *J. Appl. Polym. Sci.* **2012**, *126*, E188−E196.

(31) Hua, Y. Q.; Zhang, Y.-Q.; Wu, L.-B.; Huang, Y.-Q.; Wang, G.-Q. Mechanical and Optical Properties of Polyethylene Filled with Nano-SiO_2. *J. Macromol. Sci., Phys.* **2005**, *44*, 149−159.

(32) Mackenzie, K. J. Film and Sheeting Materials. In *Kirk−Othmer Encyclopedia of Chemical Technology*; Wiley: New York, **2000**.

(33) Smith, P. F.; Chun, I.; Liu, D.; Dimitrievich, D.; Rasburn, J.; Vancso, G. J. Studies of Optical Haze and Surface Morphology of Blown Polyethylene Films Using Atomic Force Microscopy. *Polym. Eng. Sci.* **1996**, *36*, 2129−2134.

(34) Blond, D.; Barron, V.; Ruether, M.; Ryan, K. P.; Nicolosi, V.; Blau, W. J.; Coleman, J. N. Enhancement of Modulus, Strength, and Toughness in Poly (Methyl Methacrylate)-Based Composites by the Incorporation of Poly (Methyl Methacrylate)-Functionalized Nanotubes. *Adv. Funct. Mater.* **2006**, *16*, 1608−1614.

(35) Guzmán de Villoria, R.; Miravete, A. Mechanical Model to Evaluate the Effect of the Dispersion in Nanocomposites. *Acta Mater.* **2007**, *55*, 3025−3031.

(36) Nishiyama, Y.; Langan, P.; Chanzy, H. Crystal Structure and Hydrogen Bonding System in Cellulose I$_\beta$ from Synchrotron X-Ray and Neutron Fiber Diffraction. *J. Am. Chem. Soc.* **2002**, *124*, 9074−9082.

(37) Zugenmaier, P. Characterization and Physical Properties of Cellulose Acetates. *Macromol. Symp.* **2004**, *208*, 81−166.

(38) Pakzad, A.; Simonsen, J.; Heiden, P. A.; Yassar, R. S. Size Effects on the Nanomechanical Properties of Cellulose I Nanocrystals. *J. Mater. Res.* **2012**, *27*, 528−536.

(39) Fujisawa, S.; Saito, T.; Kimura, S.; Iwata, T.; Isogai, A. Comparison of Mechanical Reinforcement Effects of Surface-Modified Cellulose Nanofibrils and Carbon Nanotubes in PLLA Composites. *Compos. Sci. Technol.* **2014**, *90*, 96−101.

(40) Songsurang, K.; Miyagawa, A.; Manaf, M. E. A.; Phulkerd, P.; Nobukawa, S.; Yamaguchi, M. Optical Anisotropy in Solution-Cast Film of Cellulose Triacetate. *Cellulose* **2013**, *20*, 83−96.

(41) Nobukawa, S.; Shimada, H.; Aoki, Y.; Miyagawa, A.; Doan, V. A.; Yoshimura, H.; Tachikawa, Y.; Yamaguchi, M. Extraordinary Wavelength Dispersion of Birefringence in Cellulose Triacetate Film with Anisotropic Nanopores. *Polymer* **2014**, *55*, 3247−3253.

(42) Turcsányi, B.; Pukánszky, B.; Tüdõs, F. Composition Dependence of Tensile Yield Stress in Filled Polymers. *J. Mater. Sci. Lett.* **1988**, *7*, 160−162.

(43) Durmus, A.; Kasgöz, A.; Macosko, C. Mechanical Properties of Linear Low-Density Polyethylene (LLDPE)/clay Nanocomposites: Estimation of Aspect Ratio and Interfacial Strength by Composite Models. *J. Macromol. Sci., Phys.* **2008**, *47*, 608−619.

(44) Demjén, Z.; Pukánszky, B.; Nagy, J. Evaluation of Interfacial Interaction in Polypropylene/Surface Treated $CaCO_3$ Composites. *Composites, Part A* **1998**, *29*, 323−329.

(45) Pukánszky, B.; Tüdõs, F.; Jancar, J.; KOLARIK, J. The Possible Mechanisms of Polymer-Filler Interaction in Polypropylene-$CaCO_3$ Composites B. *J. Mater. Sci. Lett.* **1989**, *8*, 1040−1042.

(46) Felix, J. M.; Gatenholm, P. Formation of Entanglements at Brushlike Interfaces in Cellulose-Polymer Composites. *J. Appl. Polym. Sci.* **1993**, *50*, 699−708.

(47) Százdi, L.; Pozsgay, A.; Pukánszky, B. Factors and Processes Influencing the Reinforcing Effect of Layered Silicates in Polymer Nanocomposites. *Eur. Polym. J.* **2007**, *43*, 345−359.

(48) Százdi, L.; Pukánszky, B.; Vancso, G. J.; Pukánszky, B. Quantitative Estimation of the Reinforcing Effect of Layered Silicates in PP Nanocomposites. *Polymer* **2006**, *47*, 4638−4648.

(49) Nakagaito, A. N.; Yano, H. The Effect of Fiber Content on the Mechanical and Thermal Expansion Properties of Biocomposites Based on Microfibrillated Cellulose. *Cellulose* **2008**, *15*, 555−559.

(50) Nogi, M.; Yano, H. Transparent Nanocomposites Based on Cellulose Produced by Bacteria Offer Potential Innovation in the Electronics Device Industry. *Adv. Mater.* **2008**, *20*, 1849−1852.